UNIVERSITYᴼᶠ BIRMINGHAM

Research at Birmingham

Inhibition of K+ transport through Na+, K+-ATPase by capsazepine

Mahmmoud, Yasser A; Shattock, Michael; Cornelius, Flemming; Pavlovic, Davor

Link to publication on Research at Birmingham portal

PLOS ONE

Inhibition of K$^+$ Transport through Na$^+$, K$^+$-ATPase by Capsazepine: Role of Membrane Span 10 of the α-Subunit in the Modulation of Ion Gating

Yasser A. Mahmmoud[1]*, Michael Shattock[2], Flemming Cornelius[1], Davor Pavlovic[2]

1 Department of Biomedicine, University of Aarhus, DK-8000 Aarhus C, Denmark, **2** Cardiovascular Division, King's College London, The Rayne Institute, St. Thomas' Hospital, London, United Kingdom

Abstract

Capsazepine (CPZ) inhibits Na$^+$,K$^+$-ATPase-mediated K$^+$-dependent ATP hydrolysis with no effect on Na$^+$-ATPase activity. In this study we have investigated the functional effects of CPZ on Na$^+$,K$^+$-ATPase in intact cells. We have also used well established biochemical and biophysical techniques to understand how CPZ modifies the catalytic subunit of Na$^+$,K$^+$-ATPase. In isolated rat cardiomyocytes, CPZ abolished Na$^+$,K$^+$-ATPase current in the presence of extracellular K$^+$. In contrast, CPZ stimulated pump current in the absence of extracellular K$^+$. Similar conclusions were attained using HEK293 cells loaded with the Na$^+$ sensitive dye Asante NaTRIUM green. Proteolytic cleavage of pig kidney Na$^+$,K$^+$-ATPase indicated that CPZ stabilizes ion interaction with the K$^+$ sites. The distal part of membrane span 10 (M10) of the α-subunit was exposed to trypsin cleavage in the presence of guanidinum ions, which function as Na$^+$ congener at the Na$^+$ specific site. This effect of guanidinium was amplified by treatment with CPZ. Fluorescence of the membrane potential sensitive dye, oxonol VI, was measured following addition of substrates to reconstituted inside-out Na$^+$,K$^+$-ATPase. CPZ increased oxonol VI fluorescence in the absence of K$^+$, reflecting increased Na$^+$ efflux through the pump. Surprisingly, CPZ induced an ATP-independent increase in fluorescence in the presence of high extravesicular K$^+$, likely indicating opening of an intracellular pathway selective for K$^+$. As revealed by the recent crystal structure of the E$_1$.AlF$_4$.ADP.3Na$^+$ form of the pig kidney Na$^+$,K$^+$-ATPase, movements of M5 of the α-subunit, which regulate ion selectivity, are controlled by the C-terminal tail that extends from M10. We propose that movements of M10 and its cytoplasmic extension is affected by CPZ, thereby regulating ion selectivity and transport through the K$^+$ sites in Na$^+$,K$^+$-ATPase.

Introduction

The Na$^+$,K$^+$-ATPase (sodium pump) is a heterodimeric membrane protein that pumps three sodium ions out- and two potassium ions into the cell, at the expenditure of the energy derived from hydrolysis of one ATP molecule. Consequently Na$^+$,K$^+$-ATPase establishes an electrochemical gradient for these ions across the plasma membrane, which is indispensable for many cell functions [1]. The enzyme consists of a catalytic α-subunit that undergoes ion- and ATP-dependent conformational transitions coupling ATP hydrolysis to the up-hill transport of ions. The α-subunit is associated with a glycosylated β-subunit that is important for function, folding, and plasma membrane delivery of the enzyme complex [2]. The α-subunit contains a highly conserved site for inhibition by cardiac glycosides [3]. Small auxiliary proteins belonging to the FXYD family interact with and regulate Na$^+$,K$^+$-ATPase activity in several tissues [4]. The Na$^+$,K$^+$-ATPase belongs to P$_2$-type ATPases, which includes three closely related members; sarcoplasmic reticulum Ca^{2+}-ATPase (SERCA), gastric and colonic H$^+$, K$^+$-ATPases [5].

Crystal structures of Na$^+$,K$^+$-ATPase in the two major conformations [6–9] have provided significant structure-function information. In addition, electrophysiological [10,11] and biophysical [12] measurements have proven to be pivotal to understanding the events associated with ion binding and release, as well as voltage-dependence of the pump. The mechanism of Na$^+$,K$^+$-ATPase is described by the Post-Albers scheme, which involves binding of three Na$^+$ ions from the cytoplasmic side (E$_1$ form), providing the trigger for phosphoryl transfer and formation of E$_1$P(3Na$^+$). The three Na$^+$ ions are generally considered to be first released to the extracellular side in a sequential manner from E$_2$P(3Na$^+$) [10] and then 2K$^+$ bind at the extracellular side, where K$^+$ occlusion stimulates phosphoenzyme hydrolysis, and hence E$_2$(2K$^+$) is formed. K$^+$ release to the cytoplasm and shift to the E$_1$ form is facilitated by ATP. In contrast to SERCA1a [5], crystal structures of the Na$^+$,K$^+$-ATPase revealed that the C-terminal tail of the α-subunit has a unique position, interacting with the ion binding core [7,9]. The recent structure of the E$_1$.AlF$_4$.ADP.3Na$^+$ form indicates that the C-terminal tail functions as a controller of the movement of M5 [9]. Mutational studies have shown that the C-terminal tail plays an important role in the regulation of Na$^+$ interaction from both sides of the membrane [13]. In this regard, mutations in this domain have been shown to stabilize ion

occlusion at the shared sites [14] and also to modify ion interaction with the Na^+ unique site [15].

We have previously documented an unprecedented mode of sodium pump inhibition. Capsazepine (CPZ), a synthetic transient receptor potential vanilloid antagonist [16], inhibits K^+-dependent ATP hydrolysis with no effect on Na^+-ATPase (see below) activity [17]. CPZ treatment of Na^+,K^+-ATPase was found to strongly modify nucleotide interaction with the pump and stabilize K^+ occlusion without affecting $^{22}Na^+$ influx through inside-out pumps reconstituted in lipid vesicles [17]. Hence it was concluded that CPZ blocks the K^+ transport half-cycle through the pump, leaving a Na^+ half-cycle intact. Such deviation from normal transport mode is likely a consequence of modified ion binding, raising the interesting possibility that the Na^+ specific site may function independently of the shared sites; thereby pump stoichiometry may be modulated. In support of this idea, early studies have reported a decrease in the coupling ratio of the pump in the presence of low cytoplasmic Na^+ concentrations (Ref. [18], and see Discussion). In addition, several spontaneous pump mutants were identified in disease; kinetic analyses of some of these mutants revealed a severely modified binding of Na^+ with no effect on the K^+ interaction [19]. Sodium-dependent activity is a partial reaction of the Na^+,K^+-ATPase that occurs in the absence of external K^+ [20], referred to as Na^+-ATPase activity, where Na^+, Na^+-exchange is believed to occur at $3Na^+:2\ Na^+$ stoichiometry. Na^+ replaces extracellular K^+ but with low affinity, and hence the maximum velocity of Na^+-ATPase is typically 5–15% of Na^+,K^+-ATPase in most preparations.

In this study, we present novel information on the modification of Na^+,K^+-ATPase by CPZ. First, the inhibition of pump mediated K^+ transport and stimulation of Na^+ transport (in the absence of extracellular K^+) was tested and confirmed using different experimental setups; namely, by measuring 1) whole cell sodium pump current in isolated cardiomyocytes, and 2) dynamic changes in intracellular Na^+ concentration using the dye Asante NaTRI-UM green II (ASG II). We have also performed hydrolytic activity measurements and proteolytic cleavage experiments to investigate ion-dependent conformational changes. Finally, oxonol VI, a membrane potential probe, was used to investigate the effect of CPZ on pump mediated charge movements. These different experimental approaches were all employed to shed light on the possible mechanism of action of this drug. Our data, in combination with prior mutagenesis studies, strongly suggest an uncoupled mode of the Na^+,K^+-ATPase in which movement of M10, which carries the C-terminal tail, blocks K^+ transport but allows Na^+ efflux.

Materials and Methods

Cell isolation and culture of adult rat ventricular myocytes

Animals were maintained humanely in compliance with the "Principles of Laboratory Animal Care" formulated by the National Society for Medical Research and the Guide for Care and Use of Laboratory Animals prepared by the National Academy of Sciences and published by the National Institutes of Health (NIH Pub. No. 85–23, revised 1985). All animal protocols were approved both by the local King's College Ethical Review Process Committee and by the UK Government Home Office (Animals Scientific Procedures Group). Animals were anesthetized with sodium pentobarbital in combination with sodium heparin (200 mg· kg^{-1} and 200 IU· kg^{-1}, respectively). Ventricular myocytes (ARVM) were isolated from the hearts of adult male Wistar rats (200–250 g, B&K Universal) by standard collagenase

enzymatic digestion as described earlier [21]. In all of the electrophysiology experiments, myocytes were used two hours post-isolation.

Electrophysiology

Adult rat ventricular myocytes were voltage-clamped and Na^+/K^+ pump current (I_p) was recorded at 35°C using the whole-cell ruptured-patch technique as described previously [21–23]. Briefly, myocytes were studied under whole-cell voltage-clamp using electrodes which had resistances of 1–2 MΩ when filled with (in mM) 95 $CsCH_3O_3S$, 25 $NaCH_3O_3$, 20 CsCl, 1 $MgCl_2$, 1.5 $CaCl_2$, 10 HEPES, 5 EGTA, 5 MgATP, 5 creatine phosphate pH 7.2. External solution was (in mM) 140 NaCl, 1 $MgCl_2$, 2 $NiCl_2$, 1 $BaCl_2$, 5 KCl, 10 Glucose, 10 HEPES, pH 7.2 at 35°C. The solution with either dimethyl sulfoxide (DMSO) vehicle or 30 µM CPZ was flowing at a rate of 3 ml·min^{-1}. Cell capacitance was measured from the capacitance transient generated on application of a voltage step from the holding potential of −90 mV to −80 mV. Current generated was recorded via an Axopatch 200A amplifier and pClamp10 software (Molecular Devices, California, U.S.A). Passive K^+ currents are routinely blocked by replacing intracellular K^+ with pipette Cs and by the addition of 1 mM Ba^{2+} to the extracellular solution.

Intracellular Na^+ fluorescence measurements

For measurement of changes in intracellular Na^+ a similar protocol was employed as described previously [24]. HEK293 cells were plated in black 96 well ViewPlate (PerkinElmer Inc., USA) and cultured in Dulbecco's Modified Eagle Medium (DMEM) in the presence of 10% fetal calf serum and antibiotics (100 IU ml^{-1} of penicillin and 100 µg·ml^{-1} streptomycin) until confluent. DMEM was replaced with Tyrode (in mmol/L: 140 NaCl, 4 KCl, 1 $MgCl_2$, 1 $CaCl_2$, 10 HEPES, and 10 glucose, pH 7.4) and HEK293 cells loaded for 2 hours with 5 µM of the sodium fluorophore ASG II (Teflabs Inc., USA), in the presence of the non-ionic surfactant Pluronic F-127 (0.05% w/v). External fluorophore was then washed out and cytosolic fluorophore was allowed to de-esterify for 20 min before proceeding with intracellular Na^+ measurements. HEK293 cells were de-esterified in Tyrode solution and the effects of CPZ on intracellular Na^+ examined in either K^+-free (in mmol/L: 140 NaCl, 2 EGTA, 10 HEPES, and 10 glucose, pH 7.4) or K^+-containing solution (in mmol/L: 140 NaCl, 4 KCl, 2 EGTA, 10 HEPES, and 10 glucose, pH 7.4). Single excitation (485 nm) single emission (535 nm) (dichroic 515 nm) measurements were performed using a Gemini XPS Fluorescence Microplate Reader (Molecular Devices, USA), at room temperature. Fluorescence signal decline represents overall Na^+ efflux, whereas, an increase in fluorescence signal represents Na^+ influx [24,25].

Na^+,K^+-ATPase preparation and hydrolytic activity

Plasma membranes from pig kidney red outer medulla were isolated according to a modified Jørgensen's Materials and Methods described earlier [26]. In brief, minced tissue pieces were homogenized in 30 mM imidazole buffer pH 7.4, containing 250 mM sucrose and 1 mM EDTA. The homogenate was subjected to several differential centrifugation steps to obtain a microsomal plasma membrane fraction. Microsomes were treated with a mild concentration of sodium dodecyl sulphate (SDS) to open sealed vesicles and dissociate several peripheral proteins from the membrane. The final preparation had a specific activity of 1.8–2.2 mmol.h^{-1}.mg^{-1} protein at 37°C. Protein concentration was determined using a BioRad detergent compatible kit (Cat# 500–0113), according to the manufacturer's instructions. ATPase

activity was measured by incubating the enzyme with buffer and substrates (see separate figure legends) at 24°C followed by measuring phosphate liberated from ATP, according to the method of Baginsky [27]. Control activities were measured in identical conditions but in the presence of 1 mM ouabain. For the temperature effect and vanadate sensitivity measurements, a sigmoid dose-response function was used:

$$y = bottom + \frac{top - bottom}{1 + 10^{((\log IC50 - x) \cdot Hillslope)}}$$

IC50 is the agonist concentration that gives a response halfway between top and bottom.

Para-nitrophenyl phosphatase (*p*NPPase) activity was measured in a reaction mixture containing 30 mM histidine buffer, 5 mM MgCl, 10 mM *p*NPP (disodium salt), 5 µg protein, and 100 mM of either NaCl or KCl. The pH was adjusted using Tris-HCl. The reactions were stopped with 4.5% trichloroacetic acid (TCA). Ouabain sensitive *para*-nitrophenol release was determined using a colorimetric method, by measuring the absorbance of the post-hydrolytic mixture at 410 nm. *para*-nitrophenol has a molar extinction coefficient of $1.8 \cdot 10^4 \ M^{-1} \cdot cm^{-1}$.

Proteolytic cleavage, gel electrophoresis, and immunoblotting

Controlled proteolysis of the pig kidney α-subunit was performed in a reaction mixture containing 100 µg of purified membrane protein suspended in 25 mM histidine pH 7.0 in the presence of different additions as described in figure legends. The protein was preincubated for 30 min at 24 °C before the addition of 2 µg of proteinase K (PK), and the mixtures were incubated for 45 min. Proteolysis was terminated with an equal volume of SDS sample buffer containing 1% TCA to irreversibly inhibit the protease. Cleavage with trypsin was performed in the same way but buffers with different pH values were used. The mixtures were analyzed by SDS-PAGE overnight at 150 V and 12 mA per gel. 10 µg of protein was loaded onto 8% SDS-PAGE, and protein fragments on the gel were transferred to polyvinylidene fluoride (PVDF) membranes and visualized by Western blotting using a C-terminal α-subunit antibody [raised against peptide I1002-Y1016 of the pig kidney α-subunit], as described previously [28]. Trypsin [29] and PK [30] cleavage patterns of the Na+,K+-ATPase α-subunit were previously characterized. We have produced new affinity-purified antibody raised against the last 5 C-terminal residues of the α-subunit (KETYY).

Reconstitution of Na+,K+-ATPase

Reconstitution of Na+,K+-ATPase was performed as described previously [31]. Phosphatidyl choline/cholesterol vesicles containing shark Na+,K+-ATPase were prepared in 30 mM histidine buffer pH 7, 2 mM MgCl₂, and either 30 mM NaCl alone or together with 30 mM KCl. Following treatment with $C_{12}E_8$ (detergent:protein ratio of 2:1) and isolation of the solubilized protein by centrifugation, the soluble protein was mixed with phosphatidyl choline/cholesterol in $C_{12}E_8$ and liposomes were formed by overnight incubation with biobeads to remove the detergent.

Fluorescence measurements

A SPEX Fluorolog-3 spectrofluorometer equipped with a thermostated cell compartment (23°C) and a magnetic stirrer was used to measure changes in membrane potential across liposomal membrane [30,32]. 50 µl proteoliposomes were added

to 3 ml cuvette containing 30 mM histidine buffer pH 7.2, 2 mM MgCl₂, 75 µM ATP, 0.5 µM oxonol VI, as well as other additions (see figure legends). The ATP powered increase in fluorescence emission at 660 nm (slit width 5 nm), indicative of ion transloca-tion across the membrane, is detected following excitation of the dye at 580 nm (slit width 20 nm). Data were analyzed using a one-phase association function:

$$y = y_o + (plateau - y_o) \cdot (1 - e^{-(k \cdot x)})$$

k denotes the rate constant of the reaction.

Statistical analysis

Quantitative electrophysiology data are shown as mean ± standard error of the mean (SEM) of measurements derived from cells isolated from at least 6 individual hearts. Differences between experimental groups were tested by one-way ANOVA followed by a Bonferroni post-hoc test or by unpaired *t*-tests. Differences were considered significant at $p < 0.05$. Proteolytic cleavage experiments were performed four times, with a representative result shown.

Results

Effects of CPZ on pump current in rat cardiomyocytes

In order to investigate the functional effects of CPZ on Na+,K+-ATPase activity in a more integrated system, pump current (I_p) was measured in single freshly isolated adult rat ventricular cardiomyocytes using a whole-cell ruptured patch clamp tech-nique [22,23]. I_p was defined as current inhibited by removal of extracellular K+ (K+-dependent current). I_p was measured in Tyrode solution followed by treatment with either DMSO vehicle control or 30 µM CPZ. Perfusion of the cardiomyocytes with solution containing CPZ decreased K+-dependent current, as shown in Fig. 1A. Five min of perfusion with CPZ decreased I_p by 52% (I_p decreased from 2.246 ± 0.171 to 1.172±0.1607 pA/pF; p<0.05, n = 11), whereas, 10 min of perfusion with CPZ resulted in 85% inhibition (I_p = 0.3250±0.2136 pA/pF; p<0.05, n = 7), as shown in Fig. 1B.

In the absence of extracellular K+, the activity of the enzyme is confined to Na+ translocation steps in which extracellular Na+ acts like K+ by binding to the extracellular sites. In most systems, Na+, Na+ exchange occurs at a significantly lower rate (~5–15%) compared to Na+, K+ exchange, owing to the difference in affinity between Na+ and K+ at the extracellular sites [20]. Interestingly, in the absence of extracellular K+, CPZ perfusion resulted in a small but significant increase in K+-independent I_p (Fig. 1C). This increase appears to occur on a faster timescale than the concomitant decrease in K+-dependent current (defined as K+-dependent I_p minus K+-independent I_p). The effects of CPZ on I_p is reversible; washing off the CPZ with control solution partially restored K+-dependent I_p and reduced increase in K+-independent I_p, as demonstrated by changes in I_p (shown to the left of each K+ to K+-free steps in Fig. 1D).

In order to determine whether the increase in K+-independent I_p (Fig. 1C) is ouabain-sensitive, stimulation of K+-independent I_p by CPZ was allowed to occur and then ouabain (10 mM) was added. Ouabain completely inhibited the CPZ-induced increase in K+-independent I_p (Fig. 2).

Effects of CPZ on intracellular Na+

The effects of CPZ on intracellular Na+ were examined in human embryonic kidney cells (HEK293) loaded with a Na+ sensitive dye, ASG II, using fluorescence spectroscopy [24,25].
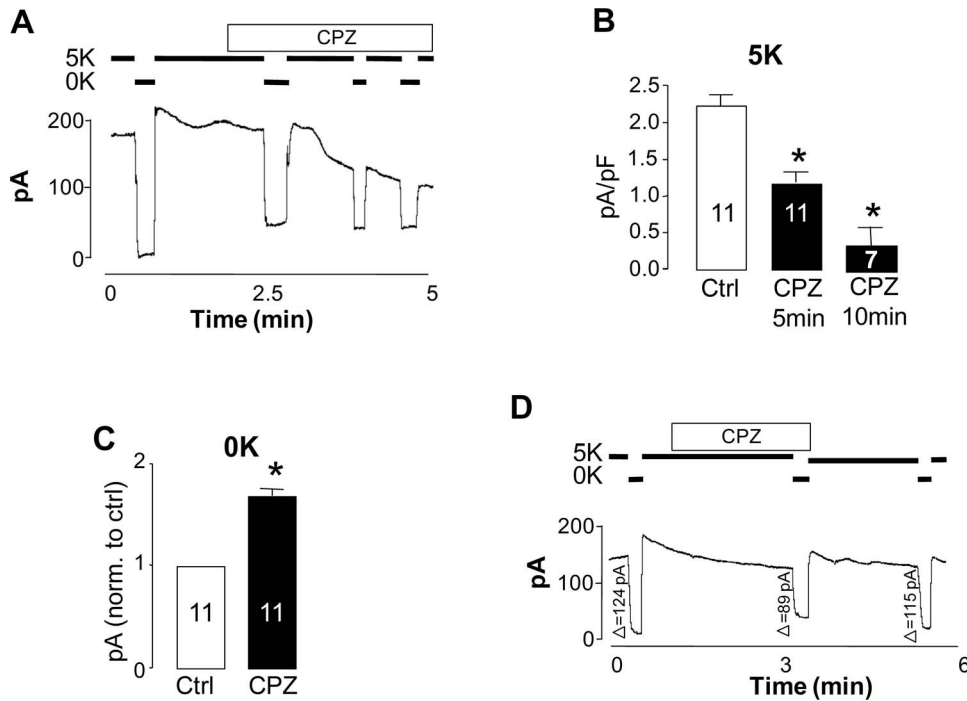
Figure 1. CPZ decreases K$^+$-dependent Na$^+$, K$^+$-ATPase transport activity. A. Raw trace of the effects of 30 μM of CPZ on Na$^+$, K$^+$-ATPase I$_p$ in adult rat cardiac myocytes. The horizontal bold lines indicate the addition and wash-off of 5 mM KCl or the addition of CPZ, as indicated. **B.** Steady state current obtained following 5 and 10 min incubation with CPZ, compared to controls not treated with CPZ. **C.** Changes in K$^+$-independent I$_p$ following the addition of CPZ. **D.** The CPZ-induced changes of Na$^+$, K$^+$-ATPase I$_p$ in adult rat cardiac myocytes are reversible. The data represent cells isolated from at least 6 individual animals, (number of cells shown inside bars; 1 min time point not shown) and are expressed as mean ±SEM (*significantly different from control, $P<0.05$). Differences between experimental groups were tested by one-way ANOVA followed by a Bonferroni post-hoc test in panel B and by unpaired t-test in panel C.
doi:10.1371/journal.pone.0096909.g001

Fluorescence of ASG II increases linearly with intracellular Na$^+$ over a physiological intracellular Na$^+$ range 0–40 mM in primary astrocytes [33] and HEK293 cells (data not shown). In the presence of an extracellular K$^+$ concentration of 4 mM (Fig. 3A), CPZ produced a dose-dependent increase in ASG II fluorescence compared to DMSO controls (~170% following treatment with 30 μM CPZ over a 60 min period), consistent with increased intracellular Na$^+$. This result is expected as CPZ was shown to inhibit coupled K$^+$-dependent activity (Fig. 1) and hence the major

route of Na$^+$ extrusion from these cells is inhibited. In the absence of extracellular K$^+$, the normal Na$^+$/K$^+$ translocation via the pump is inhibited and hence intracellular Na$^+$ inevitably rises. In the absence of K$^+$, however, CPZ reduced the rate of intracellular Na$^+$ increase in a dose-dependent manner (Fig. 3B). This result is consistent with increased uncoupled Na$^+$ efflux from cells as shown in Figs. 1C and 2.
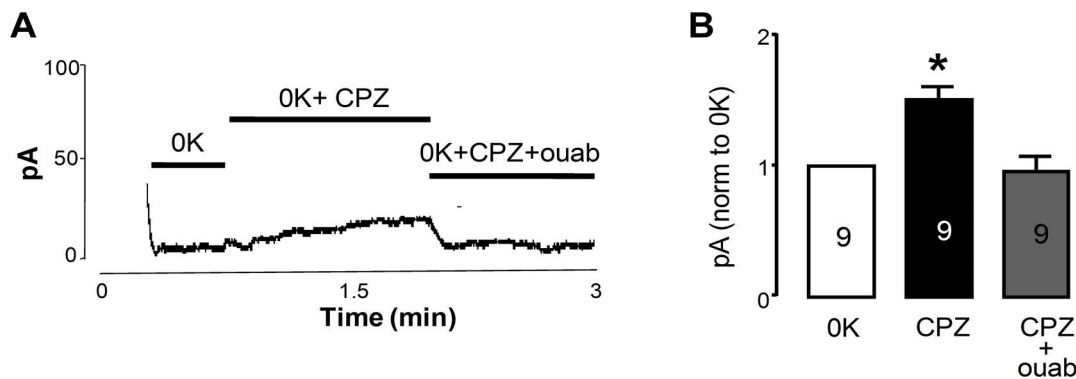
Figure 2. CPZ increases K$^+$-independent Na$^+$, K$^+$-ATPase activity. A. Raw trace of the effects of treatment with 30 μM of CPZ on K$^+$-independent I$_p$ followed by the addition of 10 mM ouabain. **B.** Changes in steady state K$^+$-independent I$_p$ as a result of CPZ and CPZ plus ouabain, normalized to the K$^+$-free control I$_p$. The data represent cells isolated from 6 individual animals [number of cells are shown inside bars] and are expressed as mean ±SEM (*significantly difference from control, $P<0.05$). Differences between experimental groups were tested by one-way ANOVA followed by a Bonferroni post-hoc test.
doi:10.1371/journal.pone.0096909.g002
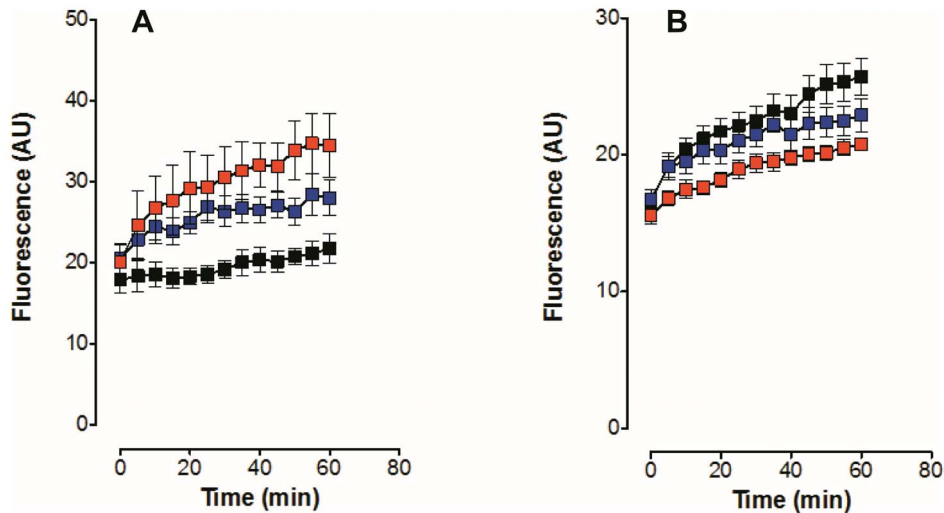
Figure 3. Effect of CPZ on ASG II fluorescence in cultured HEK293 cells. Cultured cells were suspended in Tyrode buffer and loaded with ASG II prior to fluorescence measurements, as described in Materials and Methods. Fluorescence was measured at 535 nm in the presence of 4 mM K^+ (A), or in the absence of K^+ (B) on the extracellular side. Extracellular Na^+ was 140 mM in both cases. Fluorescence, indicative of changes in intracellular Na^+ concentration, was measured as a function of time, following treatment of cells with DMSO (black squares), 10 μM CPZ (blue squares), or 30 μM CPZ (red squares).
doi:10.1371/journal.pone.0096909.g003

Effect of temperature, pH, and vanadate sensitivity of the CPZ modified enzyme

CPZ inhibition curves were measured at different temperatures, showing that temperature strongly influences CPZ inhibition (Fig. 4A). The IC50 values for CPZ inhibition were 108.2±1.31 μM, 37.33±1.08 μM, 13.88±1.05 μM, and 7.64±1.14 μM at 37°C, 30°C, 15°C, and 5°C, respectively.

Previously, we have shown that Na^+-ATPase activity is insensitive to CPZ [17]. We now demonstrate that Na^+-ATPase activity is inhibited by CPZ at basic pH but not when the pH is neutral or acidic (Fig. 4B).

Vanadate sensitivity was studied to gain information on the conformational equilibrium of the pump [28]. Orthovanadate is a transition state analogue of inorganic phosphate that binds

preferentially to the E_2 conformation of P-type ATPases. Thus, the sensitivity of Na^+,K^+-ATPase to inhibition by vanadate reflects the proportion of the enzyme adopting an E_2 conformation. Vanadate inhibition of the control enzyme followed a sigmoid curve. Analysis using the Hill equation indicated an IC_{50} for vanadate inhibition of 0.205±0.02 μM (Fig. 4C, squares). After treatment with CPZ a substantial decrease in vanadate sensitivity was observed (Fig. 4C, circles). The IC_{50} of inhibition by vanadate in the presence of CPZ was 3.43±1.05 μM. This 17 fold increase in IC_{50} indicates a CPZ-mediated strong stabilization of an E_1-like conformation.
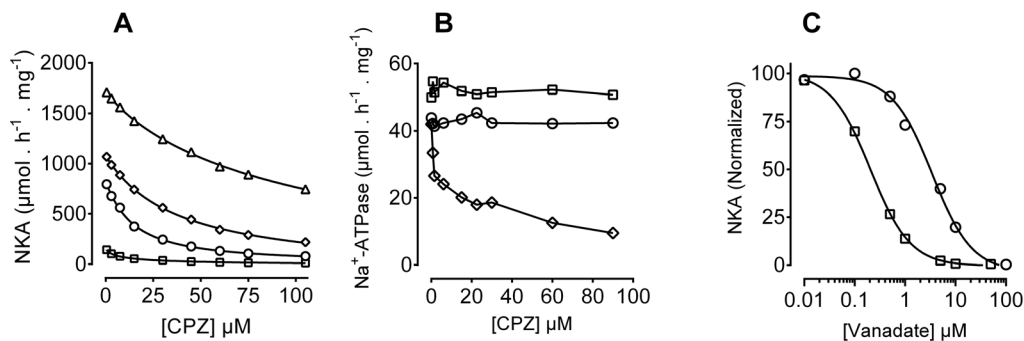
Figure 4. Effect of temperature, pH, and vanadate sensitivity of the CPZ treated enzyme. A. Pig kidney Na^+,K^+-ATPase activity was measured at four different temperatures, as described in Materials and Methods, in the presence of the indicated CPZ concentrations. The reaction contained 30 mM histidine buffer, pH 7.2, 100 mM NaCl, 20 mM KCl, 3 mM $MgCl_2$, and 3 mM ATP. The inhibition curves were analyzed using the Hill equation, giving the following IC50 values; squares, 5°C (7.64±1.14 μM); circles, 15°C (13.88±1.05 μM); diamonds, 30°C (37.33±1.08 μM); and triangles, 37 °C (108.20±1.31 μM). **B.** Effect of pH on CPZ inhibition of Na^+-ATPase activity. Na^+-ATPase activity was measured as described in panel A, but in the absence of K^+ and in the presence of different pH values (the reaction was buffered with 30 mM Tris adjusted with HCl), in the presence of the indicated CPZ concentrations. Squares, circles, and diamonds indicate measurements performed at pH 6, 7, or 8, respectively. **C.** Na^+,K^+-ATPase (NKA) activity was measured as in panel A, but in the presence of 1 mM ATP and the indicated vanadate concentrations at 23°C. The ATPase mixture contained either DMSO (squares) or 20 μM CPZ (circles).
doi:10.1371/journal.pone.0096909.g004

CPZ inhibits K$^+$-pNPPase but stimulates pNPP hydrolysis in the presence of Na$^+$

Na$^+$,K$^+$-ATPase hydrolyses pNPP in a partial reaction involving an E$_2$ form, and is detected following incubation of the enzyme in the presence of K$^+$ (E$_2$K$^+$ form), or in the presence of Na$^+$ and MgATP (E$_2$P form). pNPP hydrolysis is inhibited by ligands that stabilize the E$_1$ conformation and is therefore not observed when Na$^+$ substitutes K$^+$. We have now found that CPZ stimulates pNPP hydrolysis in the presence of 100 mM Na$^+$ and in the absence of K$^+$ (Fig. 5A). The maximum level of stimulation was independent of pH although the apparent affinity of inhibition by CPZ decreased at basic pH. Linoleic acid, a free fatty acid that stabilizes the E$_2$ conformation [32], does not produce a similar effect (Fig. 5A, closed circles). On the other hand, K$^+$-dependent pNPPase is inhibited by CPZ at all pH values tested, but the inhibition was found to be strongly dependent on pH (Fig. 5B); the apparent affinity of inhibition by CPZ was much higher at basic pH compared to acidic and neutral pH.

Cleavage with Proteinase K

Cleavage with PK of the cytoplasmic domains of the α-subunit was used as a tool to investigate the effect of CPZ on the conformation of pig kidney Na$^+$,K$^+$-ATPase. In the presence of occluded ions, a specific cleavage pattern is obtained as proteolytic sites at distinct locations are protected and others are exposed. In the absence of occluded ions, this protection is absent and all of the cytoplasmic domains of the α-subunit are completely cleaved. To this end, membrane-bound enzyme was incubated in the presence of different ion combinations with and without 50 μM CPZ, before the addition of PK (Fig. 6). Fragments were separated by SDS-PAGE and visualized by Western blotting using a specific antibody to the C-terminus of the α-subunit. In control samples, the C-terminal half of the α-subunit (a fragment of 55 kDa starting at an area close to the phosphorylation site in the P domain to the C-terminal end of the α-subunit), containing M5-M10, is accumulated in the presence of K$^+$ alone, whereas in the presence of Na$^+$ or Na$^+$ and K$^+$, the level of the 55 kDa fragment was largely reduced (Fig. 6, compare lanes labeled Na$^+$, K$^+$, and Na$^+$

plus K$^+$). Parallel experiments where cleavage products were stained with Coomassie blue indicated that the 55 kDa is almost completely cleaved to smaller fragment (data not shown). This indicates that the C-terminal half of enzyme incubated in the presence of Na$^+$ alone is less stable compared to the K$^+$-bound enzyme, and that the presence of Na$^+$ together with K$^+$ abrogates the protection provided by K$^+$. In samples treated with CPZ and then subjected to PK cleavage, in contrast, the 55 kDa fragment was protected in the presence of Na$^+$ alone or in the presence of Na$^+$ and K$^+$. In addition, CPZ treatment exposed a K$^+$-specific new cleavage site that produced a 35 kDa fragment. The 35 kDa fragment is likely a result of cleavage of the 55 kDa fragment at the area connecting the N and P domains [30]. Finally, in the presence of ADP which stabilizes a compact cytoplasmic headpiece structure, the α-subunit was protected in the presence of either Na$^+$ or K$^+$ and CPZ still had an appreciable protecting effect.

Trypsin cleavage

We sought to gain more information on the conformation of the control and CPZ modified enzymes by employing trypsin digestion, which produces well-defined cleavages at specific sites in the α-subunit in the presence of either Na$^+$ or K$^+$ ions [29]. Hence, we determined the cleavage patterns of the pig kidney α-subunit at different pH, and in the presence of 50 mM of Na$^+$, K$^+$ or guanidinium ions (Gua$^+$). Gua$^+$ derivatives have earlier been shown to antagonize Na$^+$ binding to Na$^+$,K$^+$-ATPase [34,35]. Gua$^+$ was later employed to investigate cation selectivity of the Na$^+$,K$^+$-ATPase. From electrical measurements it has been hypothesized that Gua$^+$ is accommodated in the third Na$^+$ site, as it produces voltage-dependent inhibition of an outward current in the presence of extracellular K$^+$ and it permeates through the Na$^+$ unique site, producing inward current at negative membrane
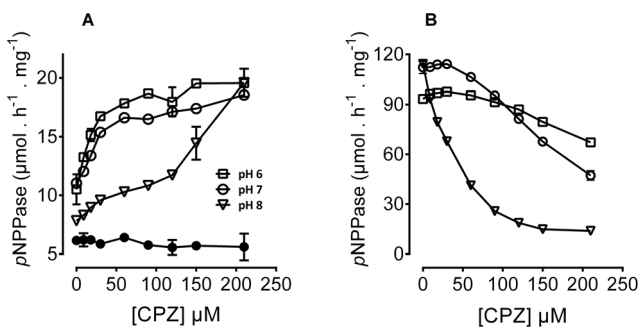
Figure 5. Effect of CPZ on pNPP hydrolysis by Na$^+$,K$^+$-ATPase. pNPPase activity was measured in the presence of histidine buffer (with the pH adjusted with Tris/HCl), 10 mM MgCl$_2$, 10 mM Na$_2^+$-pNPP, 100 mM NaCl (A) or 100 mM KCl (B) in the presence of the indicated CPZ concentrations and in the absence of ATP. Released pNP was measured in a spectrophotometer at 410 nm as described under Materials and Methods. Data are expressed as μmol hydrolyzed pNPP · h^{-1} · mg^{-1} (at 24°C). The black circles depict the effect of linoleic acid on pNPPase activity in the presence of 100 mM Na$^+$ at concentrations identical to those of CPZ. Note that the residual activity seen in panel B at high CPZ concentrations is likely due to the presence of 20 mM Na$^+$ added with pNPP.
doi:10.1371/journal.pone.0096909.g005
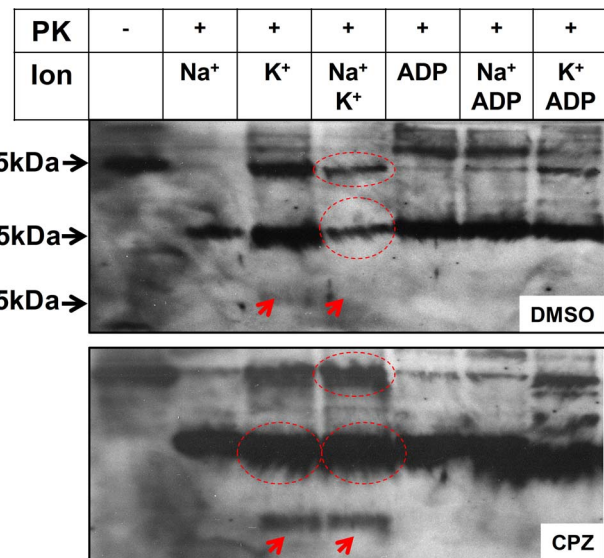
Figure 6. Proteinase K cleavage. Pig kidney membranes were incubated in 25 mM histidine buffer containing 30 mM monovalent ion, and/or 1 mM ADP, as indicated. The samples were treated with PK (PK/protein ratio ~1:50) and the mixture incubated for 40 min at 24°C, and terminated with SDS sample buffer acidified with TCA. Proteolytic products were separated using SDS-PAGE and protein fragments on the gel were transferred to PVDF membranes and visualized by Western blotting using NKA1012-1016 antibody. The labels to the left indicate the apparent molecular weights of the fragments, determined by the use of Precision plus protein standards from Bio-Rad, Cat#161-0363.
doi:10.1371/journal.pone.0096909.g006

potentials. These two features characterize Na^+ interaction with a high field access channel in the pump [36,37] and hence Gua^+ is thought of as a Na^+ congener at the Na^+ specific site.

In the presence of Na^+, cleavage at both T_3 and T_1 sites [29] occurred, whereas cleavage occurred almost exclusively at T_1 in the presence of K^+ (Fig. 7). Gua^+ produced cleavage preferentially at T_3, i.e. a similar cleavage pattern as expected for the $E_1(Na^+)$ form [29]. A conformation with exposed T_3 and substantially protected T_1 is apparently a novel one stabilized by Gua^+ binding. Importantly, in the presence of Gua^+, a short peptide was exposed to cleavage by trypsin especially at pH 8 (site T_4). This fragment is derived from the C-terminus of the α-subunit, as evidenced from its positive reaction with the KETYY antibody. Edmann degradation of this short peptide after excision from PVDF membranes yielded the sequence "^{1006}PGGXVE", a sequence immediately preceding the KETYY motif, demonstrating unambiguously that the fragment arises from the C-terminus of the α-subunit as a consequence of trypsin cleavage. When the effect of CPZ on trypsin cleavage of the α-subunit at this domain was examined we found that CPZ increased, in a concentration-dependent manner, the exposure of the tryptic site T_4 at the C-terminus (Fig. 8). The exposure of the C-terminal tail to trypsin cleavage is specific for Gua^+ and is not observed in the presence of Na^+ (Fig. 8, and see Discussion).

Another intriguing observation is the appearance of a 19 kDa fragment in the presence of Gua^+ at pH 8 (Figs. 7 and 8). This fragment is most likely identical to a well-known C-terminal third of the α-subunit starting at N831 (see Discussion) produced by

Figure 8. Effect of CPZ on cleavage of the C-terminal tail. Trypsin treatment, SDS-PAGE, and immunoblotting were performed as in Fig. 7. The effect of CPZ on accumulation of the C-terminal fragment was investigated at pH 8 in the presence of either Na^+ or Gua^+. Note the significant difference between Na^+ and Gua^+ on the accumulation of the 55 kDa fragment, occurring at the middle of the α-subunit (T_1 site, Ref. [29]). The anomalous migration of the 4 kDa peptide is possibly due to its polar properties and its small molecular mass. Note that, due to the difference in staining intensity, the upper part of the immunoblot was made less intense.
doi:10.1371/journal.pone.0096909.g008

incubation of the membrane-bound enzyme with high trypsin concentrations at $37°C$ [38].

Oxonol VI fluorescence measurements

Investigation of changes in the fluorescence of oxonol VI was used to gain information on the effect of CPZ on Na^+ translocation via the pump. ATP-dependent transport of positive charge from the medium into the liposomal lumen, establishing an inside positive membrane potential, is detected by an increase in oxonol VI fluorescence [39]. As seen from Fig. 9A, addition of ATP in the presence of 30 mM Na^+ on both sides of the membrane ($3Na^+:2Na^+$ exchange conditions) resulted in an expected increase in fluorescence (Fig 9A, black), indicative of electrogenic Na^+ exchange with net influx of Na^+ into the liposomes through reconstituted inside-out Na^+,K^+-ATPase molecules (cellular efflux). The fluorescence level reaches a plateau as the potential difference attains a level high enough to impair Na^+ release from the $E_2P(Na^+)$ form. Addition of CPZ at the plateau phase resulted in ~100% increase in fluorescence to a new plateau. The CPZ effect was pump-mediated since CPZ produced no effect on oxonol VI fluorescence in the absence of the protein (data not shown). Furthermore, addition of CPZ before ATP did not produce any change in fluorescence (Fig. 9B); an increase in fluorescence is only observed following the addition of ATP.
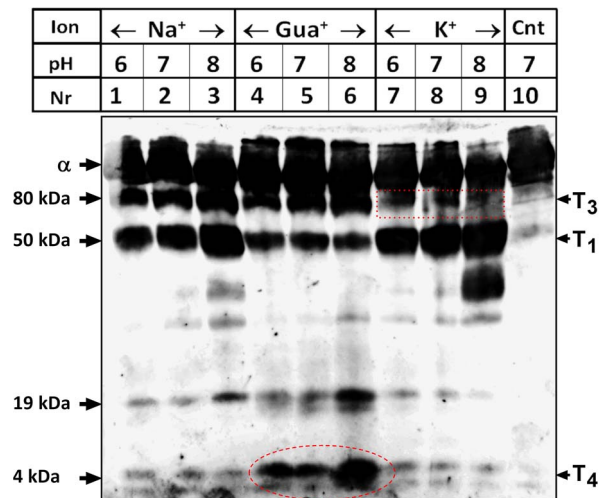

Figure 7. Trypsin cleavage in the presence of substrate ions. Trypsin cleavage of pig kidney Na^+,K^+-ATPase was performed in the presence of Tris buffer and 50 mM of NaCl, Gua^+ hydrochloride, or KCl. The enzyme (100 µg) was allowed to equilibrate with ions for 30 min at $20°C$, following by the addition of trypsin (trypsin/protein ratio ~1:100). In controls (Cnt), water replaced trypsin. The reaction was allowed to proceed for 40 min and was terminated using SDS sample buffer acidified with TCA. Protein fragments were resolved using SDS-PAGE and visualized by Western blotting using anti KETYY antibody. Each reaction was performed in the presence of Tris buffer with the indicated pH values. Representative of four different experiments is shown. The right labels indicate the symbols of cleavage sites introduced by Jørgensen [29], together with the new T_4 site. Note that the very faint bands appearing at 4 kDa in the presence of Na^+ or K^+ likely represent conformational fluctuations of the protein during incubation with the protease (Ref. [58]).
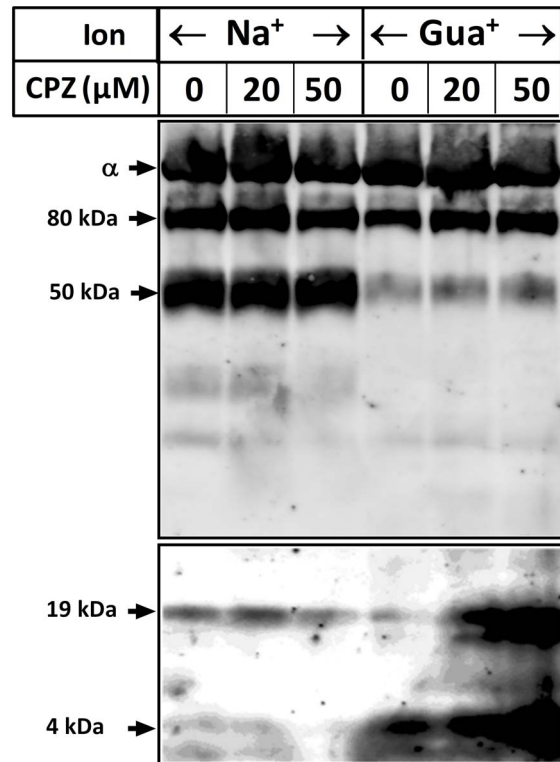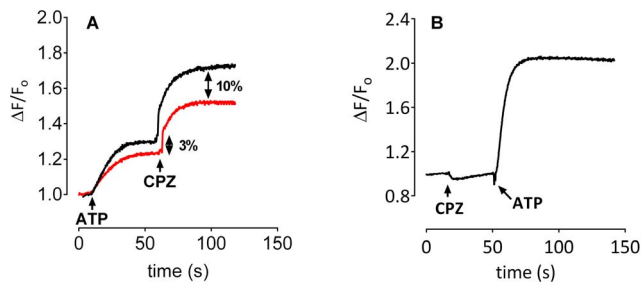doi:10.1371/journal.pone.0096909.g007

Figure 9. Effect of CPZ on oxonol VI fluorescence under Na$^+$,Na$^+$ exchange conditions. Oxonol VI fluorescence was measured as described in Materials and Methods. The working volume in the cuvette throughout the measurement was 2–2.1 ml. The cuvette contained 30 mM histidine, 30 mM NaCl, 2 mM MgCl$_2$, and 20–30 µl proteoliposomes, and the experiment was started with the addition of 75 µM ATP. After reaching steady state, 20 µM CPZ dissolved in DMSO was added. **A**. Shown is the effect of addition of ATP and CPZ in the absence (black) or in the presence (red) of 25 µM ADP. The numbers indicate the percentage decrease in maximum fluorescence occurred by pretreatment with 25 µM ADP. Representative of four independent experiments is shown. **B**. The fluorescence response was measured as in panel A, but CPZ was added first, followed by the addition of ATP, as indicated by the arrows.
doi:10.1371/journal.pone.0096909.g009

Treatment with ADP is expected to decrease the fluorescence response as it increases the backward reactions of the pump cycle by interacting with E$_1$P(3Na$^+$). Hence, the difference in fluorescence response in the absence and in the presence of ADP gives information on the approximate level of the ADP sensitive conformations. The presence of 25 µM ADP in the medium decreased the maximum fluorescence by ~3% and 10% following the addition of ATP and CPZ, respectively (Fig. 9A, red).

The experiments were also performed with liposomes produced in the presence of 30 mM Na$^+$ plus 30 mM K$^+$. After dilution in the cuvette, the extracellular side of the inside-out Na$^+$,K$^+$-ATPase (intravesicular medium) is thus exposed to 30 mM K$^+$ whereas the intracellular side (extravesicular medium) is exposed to ~100–200 µM K$^+$. 30 mM Na$^+$ was present on both sides of the membrane. Activation of inside-out Na$^+$,K$^+$-ATPase by addition of 75 µM ATP resulted in an increase in fluorescence (Fig. 10, black). However, the initial rate of fluorescence increase was significantly higher (compare to Fig. 9A) in accordance with activation of a fast 3Na$^+$:2K$^+$ exchange (phase 1) followed by a much slower phase of fluorescence increase (phase 2, Fig. 10, black). Addition of CPZ at the plateau phase produced an increase in fluorescence as observed in the absence of K$^+$ (cf. Fig. 9A, black). This seems at first paradoxical since CPZ inhibits Na$^+$,K$^+$-ATPase activity. However, after the initial activation of 3Na$^+$:2K$^+$ exchange by the addition of ATP (Fig. 10, time interval between 10 and 60 seconds on the X-axis), K$^+$ is known to be rapidly transported out of the liposomal lumen [39] and the exchange mode is likely shifted to Na$^+$ exchange. Therefore, at the time of CPZ addition the increase in fluorescence is likely due to activation of Na$^+$ efflux as with the experiments without K$^+$ (Fig. 9A). The rapid elimination of intravesicular K$^+$ is also indicated by the slow-down from the initial very fast increase in the rate of fluorescence after ATP addition to the much slower subsequent one attained after CPZ addition. Pretreatment with 25 µM ADP resulted in a significant decrease in maximum fluorescence (Fig. 10, red) compared to the decrease observed in the absence of K$^+$ (Fig. 9A, red). The maximum fluorescence levels were found to decrease by 17% and 23% following the addition of ATP and CPZ, respectively.
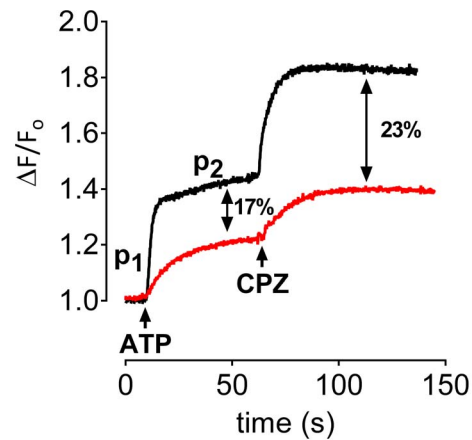

Figure 10. Effect of CPZ on oxonol VI fluorescence under Na$^+$,K$^+$ exchange conditions. Liposomes containing 30 mM NaCl, 30 mM KCl, and 2 mM MgCl$_2$ were used and the experiment was performed as in A. Extravesicular K$^+$ was diluted more than 70 folds following addition of liposomes to the medium. The ATP concentration used to start the reaction was 75 µM. The numbers indicate the percentage decrease in maximum fluorescence occurred by pretreatment with 25 µM ADP. P$_1$ and P$_2$ denote the rapid and the slow phases of fluorescence response occurring in the presence of extracellular (intravesicular) K$^+$.
doi:10.1371/journal.pone.0096909.g010

A surprising effect was observed in experiments where the effect of CPZ was studied in the presence of a high extravesicular concentration (300 mM) of either K$^+$ or Na$^+$. In the presence of a K$^+$ gradient, a substantial increase in fluorescence occurred following addition of CPZ in the absence of ATP (Fig. 11A), and subsequent addition of ATP produced only a very small increase in fluorescence. In contrast, in the presence of 300 mM Na$^+$ in the extravesicular medium, CPZ had no effect on fluorescence in the absence of ATP, whereas subsequent addition of ATP increased the fluorescence in a manner similar to that found in Fig. 9A (Fig. 11B). This CPZ effect was not influenced by the addition of digitoxigenin during a pre-incubation period of 5 min (data not shown).

Discussion

The Na$^+$,K$^+$-ATPase has been demonstrated in addition to the physiological Na$^+$:K$^+$ exchange reaction, to catalyze several partial reactions. Thus, in the absence of K$^+$, uncoupled Na$^+$ efflux, as well as electroneutral and electrogenic Na$^+$-Na$^+$ exchange have been described (For review see Refs. [40,41]). We now provide mechanistic information on a modified pump catalyzing a partial reaction-like activity in the presence of K$^+$.

CPZ inhibits active K$^+$ transport but allows Na$^+$ efflux

Patch clamp experiments (Figs. 1 and 2), ASG II (Fig. 3), and oxonol VI fluorescence measurements (Figs. 9 and 10) confirmed a model in which CPZ impairs Na$^+$/K$^+$ exchange but allows Na$^+$ efflux through the pump. In particular, ASG II data provide strong evidence that the small outward CPZ-induced current is carried by Na$^+$ and not by protons. An electro neutral shuttling of Na$^+$ on E$_1$ can be excluded since the CPZ-modified enzyme carries out electrogenic Na$^+$ transport. Under normal conditions, 3Na$^+$ leave the cell and 2K$^+$ enter. CPZ uncouples this process; K$^+$-dependent current is abolished whereas outward Na$^+$ current is increased. Hence, in CPZ-modified enzyme active Na$^+$ transport seems to be functionally independent from the K$^+$ transport
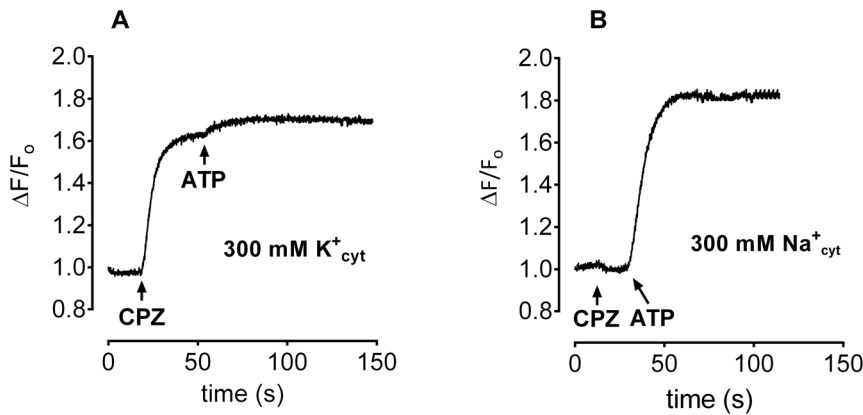
Figure 11. Effect of CPZ on oxonol VI fluorescence in the presence of 10 folds ion gradient across liposomal membrane. Liposomes were equilibrated with either 300 mM KCl (A) or 300 mM NaCl (B). The medium contained 30 mM histidine, 2 mM $MgCl_2$ and 20 μl proteoliposomes. CPZ was added first, followed by 75 μl Tris-ATP, as indicated by the arrows.
doi:10.1371/journal.pone.0096909.g011

although they share two of the three sites. Therefore, the shared sites are either blocked, or their selectivity for K^+ over Na^+ is severely increased, resulting in constitutive occupation with K^+ and inhibition of K^+-dependent hydrolytic activity. The Na^+/K^+ selectivity has been proposed to be the result of highly constrained and tightly juxtaposed Na^+ binding sites induced by binding of the first Na^+ ion to the Na^+ specific site, allowing only small Na^+ ions to bind [9]. Hence, CPZ may stabilize a similar Na^+ conformation. Based on the stabilization of K^+ occluded enzyme [17], CPZ was previously proposed to induce an E_2 variant. However, the data presented here indicate that CPZ stabilizes an E_1-like conformation, as indicated from vanadate sensitivity (Fig. 4C) and proteolytic cleavage (Figs. 7 and 8) experiments.

CPZ modulates ion interaction with the Na⁺,K⁺-ATPase

The presence of K^+ is essential in protecting the cytoplasmic domains and the 19 kDa fragment of the α-subunit from complete proteolytic cleavage [38,42], whereas Na^+ seems to provide little to no protection [43]. Furthermore, occluded K^+ ions provide more stability and protection against thermal denaturation of the membrane-bound Na^+,K^+-ATPase compared to Na^+ [44], indicating that the K^+ conformation is more stable than the Na^+ conformation. PK cleavage experiments show that the complex containing M5-M10 of the α-subunit (55 kDa fragment) is protected from cleavage in the presence of K^+ (assumed to be bound in the shared sites) but is further cleaved in the presence of Na^+ (Fig. 6). CPZ confers stability to the Na^+ bound enzyme, implying that the drug enhances binding to the shared sites of either Na^+ or K^+. Indeed, deletion of the two C-terminal tyrosine residues of the α-subunit was reported to reduce the interaction of ions with the shared sites [14]. To explain the PK data, we believe that K^+ ions bind stably in the shared sites whereas Na^+ is able to alternate between the shared sites and the Na^+ specific site. Under this condition, the shared sites may be transiently empty of ions, making the α-subunit more liable to proteolytic attack. This explanation is consistent with the well-established fact that whereas the K^+ occluded form is formed spontaneously after incubation of the dephosphorylated enzyme with K^+/Rb^+ [45], the Na^+ occluded form is not observed unless the enzyme is phosphorylated from ATP [46].

pNPPase activity is stimulated by K^+ acting from the intracellular side of the membrane [47]. Na^+ stimulates pNPP hydrolysis only in the presence of MgATP, where Na^+ is

considered to bind at the low affinity extracellular sites in the E_2P form. That Na^+ alone is incapable of stimulating pNPPase activity of the dephosphorylated enzyme implies that Na^+ cannot stably bind to the shared sites (i.e., it cannot act like K^+). The stimulation by CPZ of pNPPase activity in the presence of Na^+ alone (Fig. 5A) and in the absence of phosphorylation from ATP is in accord with the above suggestion that CPZ enhances Na^+ binding to the shared sites in a K^+ like manner, allowing for net pNPP hydrolysis, consistent with our PK data.

Gua^+ has been suggested to permeate through the Na^+ specific site [36,37]. With its large ionic radius (2.2 Å compared to 0.95 Å for Na^+), it is not possible for Gua^+ to fit in the space defining the Na^+ specific site in the $E_1 \cdot AlF_4 \cdot ADP \cdot 3Na^+$ structure. However, the size, or the exact location of the third Na^+ site may be slightly different in the $E_1 3Na^+$ conformation. Kanai et $al.$ found ~1.4 Å shift in the position of the third Na^+ in the two protomers in the crystal [9], and they have proposed that inclination of M5 would play a critical role in adjusting the size of the Na^+ specific site to only accommodate a Na^+ ion. Hence, changing the position of M5 would allow binding of ions larger than Na^+. Our tryptic cleavage experiments indicate that we are dealing with a Gua^+ "occluded" form. Incubation with trypsin in the presence of ions that are not occluded would not produce the specific cleavage pattern seen in Figs. 7 and 8. That Gua^+ alone produces an exclusive cleavage at T_3 infers that occlusion at this single site produces the conformational change defining the E_1 conformation. It is tempting to note that trypsin produces an exclusive cleavage at T_1 in the presence of K^+, whereas in the presence of Na^+ cleavage at both T_3 and T_1 is observed.

Role of the C-terminal tail

As mentioned above, changing the position of M5 would create space for the binding of larger ions to the Na^+ specific site. Indeed, the C-terminal tail was proposed to critically regulate M5 movements. In fact, M10, from which the C-terminal tail extends, contains a relatively large number of polar amino acids, indicating its loose association with the membrane. Hence, it is noteworthy to mention that temperature, which strongly affects the inhibition of the pump by CPZ (Fig. 4A), has been shown to affect movements of the C-terminal third of the α-subunit, leading to exposure of the extracellular loops between M7M8 and M9M10 [48]. Hyperthermia has even been shown to dissociate all four M7M10 membrane

spans from the membrane core to the extracellular medium [49,50].

We have provided direct evidence for a CPZ-mediated conformational change that exposes the C-terminal domain of the α-subunit to trypsin cleavage (as shown in Fig. 8) in the presence of Gua^+, an ion that was previously shown to permeate the Na^+ specific site [36,37]. Fig. 12 shows the location of the T_4 site in the crystal structure of the pig kidney enzyme in the $E_1 \cdot AlF_4^- \cdot ADP \cdot 3Na^+$ form (PDB accession nr 3WGU, Ref. [9]). The three C-terminal arginine residues, R1003-R1005, build the last C-terminal turn in M10. A similar architecture is also present in the $E_2 \cdot MgF_4^{2-} \cdot 2K^+$ structure [7]. Proteolytic data (Figs. 7 and 8) suggest that the distal part of M10 is buried in the membrane but is exposed to trypsin attack by a conformational change. The major factor that produces exposure of the C-terminal tail was found to be Gua^+. The effect of Gua^+ is enhanced by either high pH (Fig. 7) or CPZ (Fig. 8). Surprisingly, the effects seen in the presence of Gua^+ were not reproduced by Na^+. A similar paradox was indeed reported in the study by Ratheal et al. [37]; H^+ and Gua^+ were found to leak through site III in the pump whereas Na^+ did not. This is likely related to the fact that Na^+ can bind both the shared and the specific site whereas Gua^+ cannot. If binding to the shared sites controls access to the Na^+ specific site, the unique effect of Gua^+ may be reconciled.

Exposure of the C-terminal tail to trypsin cleavage could be explained if it is assumed that M10 moves toward the cytoplasm during conformational changes (see dashed arrow in Fig. 12). In principle, modifying the position of the C-terminal tail would regulate the inclination of M5 and thereby ion selectivity at the shared sites. Distortion of the K^+ sites may explain the strong modification of K^+ interaction with the pump. Whether CPZ produces direct effects on the movement of M10 is the subject of future investigations. The presence of membrane-embedded arginine residues in the distal part of the α-subunit's M10 is intriguing, as it may suggest a role of electrostatic interactions in regulating movements of the domain. Biophysical studies will be required to confirm this. Finally, it appears that the loop containing N831, cleavage at which produces the 19 kDa C-terminal fragment, is closer to the T_4 site in the structure representing the E_1 form (Fig. 12, Ref. 9) than in the structure representing the E_2 form [7]. This may explain why we see the 19 kDa fragment after cleavage at 24°C in the presence of Gua^+.

Uncoupling as an intrinsic property of P-type pumps

The uncoupling produced by CPZ could be accomplished if we assume that Na^+ in the unique site exits through a different pathway than that adopted by ions in the shared sites, allowing Na^+ transport independent of K^+ transport. Such a model is supported by literature date. Transient pump currents initiated by voltage jumps indicated that two Na^+ ions are released to the outside by a mechanism distinct from the mechanism that releases the first Na^+ [51]. Gua^+ was suggested to permeate through site III under conditions where transport through the shared sites is impaired [37]. In early studies, the coupling ratio of the pump was found to decrease from 1.5 to ∼ 0.5 at low cytoplasmic Na^+ concentrations (180 μM) and the author concluded that the enzyme can function with less than three sites filled with Na^+ [18]. Intriguingly, studies on mutants (numbering according to the pig kidney α-subunit) Glu779→Ala [52] and Phe786→Leu [53] revealed information that strongly support our conclusion. Glu779 coordinates one of the shared sites, whereas Phe786 is located close to the extracellular face of the membrane away from the ion binding sites. Both mutations mimic removal of the functional carboxyl group or the aromatic ring, respectively.
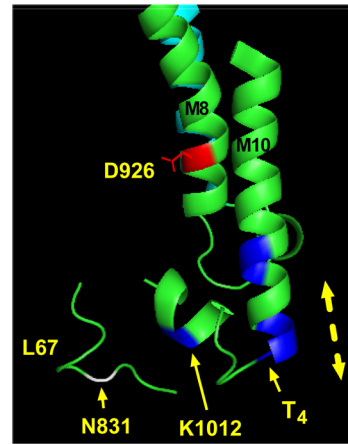

Figure 12. Proteolytic cleavage site in the E_1 structure of the Na^+,K^+-ATPase. Architecture of the cytoplasmic loop between membrane spans 6 and 7, as well as the cytoplasmic part of membrane spans 8–10 together with the C-terminal extension in the $E_1 \cdot Al$-$F_4^- \cdot ADP \cdot 3Na^+$ (PDB accession nr 3WGU). The figure was made using Pymol (www.pymol.com). D926, which coordinates Na^+ in the unique site, is shown in red. Part of the intracellular loop between membrane spans 6 and 7 (L67) is shown. This part contains an asparagine residue (N831, shown in white), cleavage at which produces the C-terminal 19 kDa fragment of the α-subunit [Ref. 38]. Positive amino acids in the C-terminal part of the α-subunit are shown in blue. T_4 indicates the cleavage site described in this study, occurring between R1005 and P1006, as evidenced from Edman degradation. Part of M9, shown in cyan, appears behind M8. The dashed double-headed arrow indicates hypothetical movements of M10 that would result in deflection of the C-terminal tail and consequently modification of the ion binding sites.
doi:10.1371/journal.pone.0096909.g012

Interestingly, these mutations produced enzyme sustaining higher Na^+-ATPase activity compared to the wild-type. Na^+ was shown to dephosphorylate the enzyme at higher rate (implying that Na^+ acts in a K^+-like manner) and K^+ inhibited ATP hydrolysis owing to unusually stable K^+ occluded enzyme. Removal of the aromatic ring of Phe786 is not expected to directly affect ion binding sites, hence, altered position of M5 likely accounts for the modified Na^+/K^+ selectivity reported earlier [53].

In the presence of a high extravesicular (intracellular) K^+ concentration, CPZ induces an electrogenic component that is ATP-independent (Fig. 11A) showing that it is not associated with active pumping. A similar response is not observed in the presence of a Na^+ gradient (Fig. 11B). This difference is quite dramatic and the question is whether this additional component is associated with enzyme mediated ion-specific passive transport across the membrane? It has previously been shown that the Na^+,K^+-ATPase provides a K^+ channel across the membrane in the presence of palytoxin [54]. However, early experiments [17] indicated that CPZ increases K^+ binding to the membranes, suggesting a modified gating mechanism involving increased rate of K^+ occlusion, or decreasing rate of K^+ deocclusion, or both. It is, therefore, inconceivable that CPZ impairs active K^+ transport by making the enzyme leaky to K^+. An explanation to the ATP-independent increase in fluorescence induced by CPZ (Figure 11A) could be the internal dipole of the ATPase itself. Membrane proteins sustaining 'active' potentials may produce responses ascribed to changes in the internal dipole of the protein, leading to redistribution of the dye molecules and hence change in fluorescence [55]. Since CPZ acts with a proton [56], addition of K^+ in the vicinity of protonated sites would increase the

fluorescence response of the negatively charged dye. Further studies are required to resolve this K^+ specific response.

In summary, we have confirmed the uncoupling of the Na^+,K^+-ATPase that results in reduction of K^+ transport with preserved or activated Na^+ transport using patch clamped myocytes and fluorescence of ASG II. The uncoupling is most likely due to modified Na^+/K^+ selectivity. In this regard, it is interesting to note that protonation of acidic residues play a significant role in determination of Na^+/K^+ selectivity of the shared sites [57]. The switch of CPZ interaction produced by shift from neutral to basic pH may suggest that CPZ itself acts differently in the protonated and deprotonated states and hence the drug exerts different effects at neutral and basic pH (Fig.4B). Although the present results cannot unequivocally discriminate between our different proposals for the CPZ effects, M10 and the tail it carries likely play a pivotal role in the CPZ dependent regulation of K^+ interaction. Further studies are warranted to investigate the molecular mechanism(s) whereby ion selectivity is regulated; especially those responsible for the active transport of K^+ into the cell.

Acknowledgments

Author Contributions

Conceived and designed the experiments: YAM MS DP. Performed the experiments: YAM MS DP. Analyzed the data: YAM FC DP. Contributed reagents/materials/analysis tools: FC. Wrote the paper: YAM. Commented on the manuscript: YAM MS DP FC.

References

1. Geering K (2008) Functional roles of Na^+,K^+-ATPase subunits. Curr Opin Nephrol Hypertens 17: 526–532.
2. Kaplan JH (2002) Na^+,K^+-ATPase. Ann Rev Biochem 71: 511–535.
3. Lingrel JB (2010) The physiological significance of the cardiotonic steroid/ouabain-binding site of the Na^+,K^+-ATPase. Ann Rev Physiol 72: 395–412.
4. Cornelius F, Mahmmoud YA (2003) Functional modulation of the sodium pump. The regulatory proteins "Fixit". News Phyiol Sci 18: 119–124.
5. Palmgren M, Nissen P (2011) P-type ATPases. Ann Rev Biophys 40: 243–266.
6. Shinoda T, Ogawa H, Cornelius F, Toyoshima C (2009) Crystal structure of the sodium-potassium pump at 2.4 Å resolution. Nature 459: 446–450.
7. Morth JP, Pedersen BP, Toustrup-Jensen MS, Sørensen TL, Petersen J, et al. (2007) Crystal structure of the sodium potassium pump. Nature 450: 1043–1049.
8. Nyblom M, Poulsen H, Gourdon P, Reinhard L, Andersson M, et al. (2013) Crystal structure of Na^+,K^+-ATPase in the Na^+-bound state. Science 342: 123–127.
9. Kanai R, Ogawa H, Vilsen B, Cornelius F, Toyoshima C (2013) Crystal structures of a Na^+ bound Na^+,K^+-ATPase preceding the E1P state. Nature 502: 201–206.
10. Holmgren M, Wagg J, Bezanilla F, Rakowski RF, De Weer P, et al. (2000) Three distinct and sequential steps in the release of sodium ions by the Na^+/K^+-ATPase. Nature 403: 898–901.
11. Takeuchi A, Reyes N, Artigas P, Gadsby DC (2008) The ion pathway through the opened Na^+,K^+-ATPase pump. Nature 456: 413–416.
12. Apell HJ, Karlish SJ (2001) Functional properties of Na^+,K^+-ATPase, and their structural implications, as detected with biophysical techniques. J memb Biol 180: 1–9.
13. Toustrup-Jensen MS, Holm R, Einholm AP, Schack VR, Morth JP, et al. (2009) The C terminus of Na^+,K^+-ATPase controls Na^+ affinity on both sides of the membrane through Arg935. J Biol Chem 284: 18715–18725.
14. Vedovato N, Gadsby DC (2010) The two C-terminal tyrosines stabilize occluded Na/K pump conformations containing Na^+ or K^+ ions. J Gen Physiol 136: 63–82.
15. Poulsen H, Khandelia H, Morth JP, Bublitz M, Mouritsen OG, et al. (2010) Neurological disease mutations compromise a C-terminal ion pathway in the Na^+/K^+-ATPase. Nature 467: 99–102.
16. Moran MM, McAlexander MA, Biro T, Szallasi A (2011) Transient receptor potential channels as therapeutic targets. Nat Rev Drug Discov 10: 601–620.
17. Mahmmoud YA (2008) Capsazepine, a synthetic vanilloid that converts the Na^+,K^+-ATPase to Na^+-ATPase. Proc Natl Acad Sci USA 105: 1757–1761.
18. Blostein R (1983) The influence of cytoplasmic sodium concentration on the stoichiometry of the sodium pump. J Biol Chem 258: 12228–12232.
19. Einholm AP, Toustrup-Jensen MS, Holm R, Andersen JP, Vilsen B (2010) The rapid-onset dystonia parkinsonism mutation D923N of the Na^+, K^+-ATPase alpha3 isoform disrupts Na^+ interaction at the third Na^+ site. J Biol Chem 285: 26245–25254.
20. Cornelius F, Skou JC (1985) Na^+, Na^+ exchange mediated by Na^+,K^+-ATPase reconstituted into liposomes. Evaluation of pump stoichiometry and responses to ATP and ADP. Biochim Biophys Acta 818: 211–221.
21. Pavlovic D, McLatchie LM, Shattock MJ (2010) The rate of loss of t-tubules in cultured adult ventricular myocytes is species dependent. Exp Physiol 95: 518–527.
22. Pavlovic D, Fuller W, Shattock MJ (2007) The intracellular region of FXYD1 is sufficient to regulate cardiac Na^+,K^+-ATPase. FASEB J 21: 1539–1546.
23. Fuller W, Howie J, McLatchie LM, Weber RJ, Hastie CJ, et al. (2009) FXYD1 phosphorylation in vitro and in adult rat cardiac myocytes: Threonine 69 is a novel substrate for protein kinase C. Am J Physiol Cell Physiol 296: C1346–C1355.
24. Pavlovic D, Hall AR, Kennington EJ, Aughton K, Boguslavskyi A, et al. (2013) Nitric oxide regulates cardiac intracellular Na^+ and Ca^{2+} by modulating Na/K ATPase via PKCε and phospholemman-dependent mechanism. J Mol Cell Cardiol 61: 164–171.
25. Despa S, Vecer J, Steels P, Ameloot M (2000) Flourescence lifetime microscopy of the Na^+ indicator Na^+ green in HeLa cells. Anal Biochem 281: 159–175.
26. Klodos I, Esmann M, Post RL (2002) Large-scale preparation of sodium-potassium ATPase from kidney outer medulla. Kid Int 62: 2097–2100.
27. Baginsky ES, Foa PP, Zak B (1967) Micro determination of inorganic phosphate, phospholipids, and total phosphate in biological materials. Clin Chim Acta 13: 326–332.
28. Mahmmoud YA, Cramb G, Maunsbach AB, Cutler CP, Meischke L, et al. (2003) Regulation of Na^+,K^+-ATPase by PLMS, the phospholemman-like protein from shark: molecular cloning, sequence, expression, cellular distribution, and functional effects of PLMS. J Biol Chem 278: 37427–37438.
29. Jørgensen PL, Collins JH (1986) Tryptic and chemotryptic cleavage sites in sequence of α-subunit of Na^+,K^+-ATPase from outer medulla of mammalian kidney. Biochim Biophys Acta 860: 570–576.
30. Cornelius F, Mahmmoud YA, Toyoshima C (2011) Metal fluoride complexes of Na^+,K^+-ATPase: Characterization of fluoride-stabilized phosphoenzyme analogues and their interaction with cardiotonic steroids. J Biol Chem 286: 29882–29892.
31. Cornelius F, Skou JC (1984) Reconstitution of Na^+, K^+-ATPase into phospholipid vesicles with full recovery of its specific activity. Biophys Biochim Acta 772: 357–373.
32. Mahmmoud YA, Christensen SB (2011) Oleic and linoleic acids are active principles in Nigella sativa and stabilize an E_2P conformation of the Na^+,K^+-ATPase. Fatty acids differentially regulate cardiac glycoside interaction with the pump. Biochim Biophys Acta 1808: 2413–2420.
33. Lamy CM, Chatton J.-Y (2011) Optical probing of sodium dynamics in neurons and astrocytes NeuroImage 58: 572–578
34. David P, Mayan H, Cohen H, Tal DM, Karlish SJD (1992) Guanidinium derivatives act as high affinity antagonists of Na^+ ions in occlusion sites of Na^+,K^+-ATPase. J Biol Chem 267: 1141–1149.
35. Or E, David P, Shainskaya A, Tal DM, Karlish SJD (1993) Effect of competitive sodium-like antagonists on Na^+,K^+-ATPase suggest that cation occlusion from the cytoplasmic surface occurs in two steps. J Biol Chem 268: 16929–16937.
36. Yaragatupalli S, Olivera JF, Gatto C, Artigas P (2009) Altered Na^+ transport after an intracellular α-subunit deletion reveal strict external sequential release of Na^+ from the Na^+/K^+ pump. Proc Natl Acad Sci USA 106: 15507–15512.
37. Ratheal IM, Virgin GK, Yu H, Roux B, Gatto C. et al. (2010) Selectivity of externally facing ion-binding sites in the Na/K pump to alkali metals and organic cations. Proc Natl Acad Sci USA 107: 18718–1872.
38. Karlish S, Goldshleger R, Stein WD (1990) A 19-kDa C-terminal tryptic fragment of the alpha chain of Na^+/K^+-ATPase is essential for occlusion and transport of cations. Proc Natl Acad Sci USA 87: 4566–4570.
39. Apell HJ, Bersch B (1987) Oxonol VI as an optical indicator for membrane potentials in lipid vesicles. Biochim Biophys Acta 903: 480–494.
40. Kaplan JH (1983) Sodium ions and the sodium pump: transport and enzymatic activity. Am J Physiol Gastrointes Liver Physiol 245: G327–G333.
41. Cornelius F (1991) Functional reconstitution of the sodium pump. Kinetics of exchange reactions performed by reconstituted Na^+,K^+-ATPase. Biochim Biophys Acta 1071: 19–66
42. Shainskaya A, Karlish SJD (1994) Evidence that the cation occlusion domain of Na/K-ATPase consists of a complex of membrane-spanning segments. Analysis of limit membrane-embedded tryptic fragments. J Biol Chem 269: 10780–10789.
43. Capasso JM, Hoving S, Tal DM, Goldshleger R, Karlish SJ (1992) Extensive digestion of Na^+,K^+-ATPase by specific and nonspecific proteases with preservation of cation occlusion sites. J Biol Chem 267: 1150–1158.
44. Kaufman SB, Luis González-Flecha F, González-Lebrero RM (2012) Opposing effects of Na^+ and K^+ on the thermal stability of Na^+,K^+-ATPase. J Phys Chem B 116: 3421–3429.
45. González-Lebrero RM, Kaufman SB, Montes MR, Nørby JG, Garrahan PJ, et al. (2002) The Occlusion of Rb^+ in the Na^+/K^+-ATPase. I. The identity of

occluded states formed by the physiological or the direct routes: occlusion/deocclusion kinetics through the direct route. J Biol Chem 277: 5910–921.

46. Glynn IM, Hara Y, Richards ED (1984) The occlusion of sodium ions within the mammalian sodium-potassium pump: its role in sodium transport. J Physiol 351: 531–554.

47. Drapeau P, Blostein R (1980) Interaction of K^+ with Na^+,K^+-ATPase. Orientation of K^+-phosphatase sites studied with inside-out red cell membrane vesicles. J Biol Chem 255: 7827–7834.

48. Donnet C, Arystarkhova E, Sweadner KJ (2001) Thermal denaturation of the Na^+,K^+-ATPase provides evidence for α-α oligomeric interaction and γ subunit association with the C-terminal domain. J Biol Chem 276: 7357–7365.

49. Goldshleger R, Tal DM, Karlish SJD (1995) Topology of the alpha-subunit of Na^+,K^+-ATPase based on proteolysis. Lability of the topological organization. Biochemistry 34: 8668–8679.

50. Arystarkhova E, Gibbons DL, Sweadner KJ (1995) Topology of the Na^+,K^+-ATPase. Evidence for externalization of a labile transmembrane structure during heating. J Biol Chem 270: 8785–8796.

51. Ding Y, Hao J, Rakowski RF (2011) Effects of oligomycin on transient current carried by Na^+ translocation of Bufo Na^+,K^+-ATPase expressed in Xenopus Oocytes. J Memb Biol 243: 35–46.

52. Vilsen B (1995) Mutant Glu781$\rightarrow$Ala of the rat kidney Na^+,K^+-ATPase displays low cation affinity and catalyzes ATP hydrolysis at a high rate in the absence of potassium ions. Biochemistry 34: 1455–1463.

53. Vilsen B (1999) Mutant Phe788$\rightarrow$Leu of the Na^+,K^+-ATPase is inhibited by micromolar concentrations of potassium and exhibits high Na^+-ATPase activity at low sodium concentrations. Biochemistry 38: 11389–11400.

54. Rossini GP, Bigiani A (2011) Palytoxin action on the Na^+,K^+-ATPase and the disruption of ion equilibria in biological systems. Toxicon 57: 429–439.

55. Cooper CE, Bruce D, Nicholls P (1990) Use of Oxonol V as a probe of membrane potential in liposomes containing cytochrome oxidase in the sub mitochondrial orientation. Biochemistry 29: 3859–3865.

56. Yamamura H, Ugawa S, Ueda T, Nagao M, Shimada S (2004) Capsazepine Is a Novel Activator of the δ Subunit of the Human Epithelial Na^+ Channel. J Biol. Chem. 279: 44483–44489.

57. Yu H, Ratheal IM, Artigas P, Roux B (2011) Protonation of key acidic residues is critical for the K^+ selectivity of the NaK pump. Nature Struc Mol Biol 18: 1159–1163.

58. Inesi G, Lewis D, Toyoshima C, Hirata A, de Meis L (2008) Conformational fluctuations of the Ca^{2+}-ATPase in the native membrane environment. Effects of pH, temperature, catalytic substrates, and thapsigargin. J Biol Chem 283: 1189–1196.